Measurement of the Branching Fraction and CP Asymmetry in $B^+ \to \rho^+ \pi^0$

J. Zhang,[7] K. Abe,[7] K. Abe,[39] T. Abe,[7] H. Aihara,[41] Y. Asano,[45] V. Aulchenko,[1] T. Aushev,[11] T. Aziz,[37] S. Bahinipati,[4] A. M. Bakich,[36] A. Bay,[16] I. Bedny,[1] U. Bitenc,[12] I. Bizjak,[12] S. Blyth,[23] A. Bondar,[1] A. Bozek,[24] M. Bračko,[18,12] T. E. Browder,[6] P. Chang,[23] Y. Chao,[23] K.-F. Chen,[23] B. G. Cheon,[3] R. Chistov,[11] S.-K. Choi,[5] Y. Choi,[35] A. Chuvikov,[31] M. Danilov,[11] M. Dash,[46] L. Y. Dong,[9] J. Dragic,[19] A. Drutskoy,[4] S. Eidelman,[1] V. Eiges,[11] Y. Enari,[20] S. Fratina,[12] N. Gabyshev,[1] A. Garmash,[31] T. Gershon,[7] G. Gokhroo,[37] B. Golob,[17,12] H. Hayashii,[21] M. Hazumi,[7] T. Higuchi,[7] L. Hinz,[16] T. Hokuue,[20] Y. Hoshi,[39] W.-S. Hou,[23] Y. B. Hsiung,[23,*] T. Iijima,[20] A. Imoto,[21] K. Inami,[20] A. Ishikawa,[7] H. Ishino,[42] R. Itoh,[7] H. Iwasaki,[7] M. Iwasaki,[41] Y. Iwasaki,[7] J. H. Kang,[47] J. S. Kang,[14] N. Katayama,[7] H. Kawai,[2] T. Kawasaki,[26] H. R. Khan,[42] H. Kichimi,[7] H. J. Kim,[15] J. H. Kim,[35] T. H. Kim,[47] K. Kinoshita,[4] P. Koppenburg,[7] S. Korpar,[18,12] P. Križan,[17,12] P. Krokovny,[1] S. Kumar,[29] A. Kuzmin,[1] Y.-J. Kwon,[47] G. Leder,[10] S. E. Lee,[34] S. H. Lee,[34] T. Lesiak,[24] J. Li,[33] A. Limosani,[19] S.-W. Lin,[23] J. MacNaughton,[10] G. Majumder,[37] F. Mandl,[10] T. Matsumoto,[43] W. Mitaroff,[10] K. Miyabayashi,[21] H. Miyake,[28] H. Miyata,[26] R. Mizuk,[11] D. Mohapatra,[46] G. R. Moloney,[19] T. Mori,[42] T. Nagamine,[40] Y. Nagasaka,[8] M. Nakao,[7] S. Nishida,[7] O. Nitoh,[44] T. Nozaki,[7] T. Okabe,[20] S. Okuno,[13] S. L. Olsen,[6] W. Ostrowicz,[24] H. Ozaki,[7] P. Pakhlov,[11] C. W. Park,[14] H. Park,[15] N. Parslow,[36] L. E. Piilonen,[46] F. J. Ronga,[7] M. Rozanska,[24] H. Sagawa,[7] Y. Sakai,[7] T. R. Sarangi,[7] O. Schneider,[16] J. Schümann,[23] A. J. Schwartz,[4] S. Semenov,[11] K. Senyo,[20] M. E. Sevior,[19] H. Shibuya,[38] B. Shwartz,[1] A. Somov,[4] N. Soni,[29] R. Stamen,[7] S. Stanič,[45,†] M. Starič,[12] K. Sumisawa,[28] T. Sumiyoshi,[43] S. Suzuki,[32] O. Tajima,[40] F. Takasaki,[7] K. Tamai,[7] M. Tanaka,[7] G. N. Taylor,[19] Y. Teramoto,[27] T. Tomura,[41] T. Tsuboyama,[7] T. Tsukamoto,[7] S. Uehara,[7] T. Uglov,[11] K. Ueno,[23] Y. Unno,[2] S. Uno,[7] G. Varner,[6] K. E. Varvell,[36] S. Villa,[16] C. C. Wang,[23] C. H. Wang,[22] M.-Z. Wang,[23] M. Watanabe,[26] Y. Watanabe,[42] B. D. Yabsley,[46] Y. Yamada,[7] A. Yamaguchi,[40] Y. Yamashita,[25] M. Yamauchi,[7] Heyoung Yang,[34] J. Ying,[30] Y. Yusa,[40] S. L. Zang,[9] C. C. Zhang,[9] Z. P. Zhang,[33] V. Zhilich,[1] T. Ziegler,[31] and D. Žontar[17,12]

(Belle Collaboration)

[1]*Budker Institute of Nuclear Physics, Novosibirsk*
[2]*Chiba University, Chiba*
[3]*Chonnam National University, Kwangju*
[4]*University of Cincinnati, Cincinnati, Ohio 45221*
[5]*Gyeongsang National University, Chinju*
[6]*University of Hawaii, Honolulu, Hawaii 96822*
[7]*High Energy Accelerator Research Organization (KEK), Tsukuba*
[8]*Hiroshima Institute of Technology, Hiroshima*
[9]*Institute of High Energy Physics, Chinese Academy of Sciences, Beijing*
[10]*Institute of High Energy Physics, Vienna*
[11]*Institute for Theoretical and Experimental Physics, Moscow*
[12]*J. Stefan Institute, Ljubljana*
[13]*Kanagawa University, Yokohama*
[14]*Korea University, Seoul*
[15]*Kyungpook National University, Taegu*
[16]*Swiss Federal Institute of Technology of Lausanne, EPFL, Lausanne*
[17]*University of Ljubljana, Ljubljana*
[18]*University of Maribor, Maribor*
[19]*University of Melbourne, Victoria*
[20]*Nagoya University, Nagoya*
[21]*Nara Women's University, Nara*
[22]*National United University, Miao Li*
[23]*Department of Physics, National Taiwan University, Taipei*
[24]*H. Niewodniczanski Institute of Nuclear Physics, Krakow*
[25]*Nihon Dental College, Niigata*
[26]*Niigata University, Niigata*
[27]*Osaka City University, Osaka*
[28]*Osaka University, Osaka*
[29]*Panjab University, Chandigarh*
[30]*Peking University, Beijing*

[31]Princeton University, Princeton, New Jersey 08545
[32]Saga University, Saga
[33]University of Science and Technology of China, Hefei
[34]Seoul National University, Seoul
[35]Sungkyunkwan University, Suwon
[36]University of Sydney, Sydney NSW
[37]Tata Institute of Fundamental Research, Bombay
[38]Toho University, Funabashi
[39]Tohoku Gakuin University, Tagajo
[40]Tohoku University, Sendai
[41]Department of Physics, University of Tokyo, Tokyo
[42]Tokyo Institute of Technology, Tokyo
[43]Tokyo Metropolitan University, Tokyo
[44]Tokyo University of Agriculture and Technology, Tokyo
[45]University of Tsukuba, Tsukuba
[46]Virginia Polytechnic Institute and State University, Blacksburg, Virginia 24061
[47]Yonsei University, Seoul

(Received 2 June 2004; published 24 January 2005)

We report a measurement of the branching fraction for the decay $B^+ \to \rho^+ \pi^0$ based on a 140 fb^{-1} data sample collected with the Belle detector at the KEKB asymmetric e^+e^- collider. We measure the branching fraction $\mathcal{B}(B^+ \to \rho^+ \pi^0) = (13.2 \pm 2.3(\text{stat})^{+1.4}_{-1.9}(\text{syst})) \times 10^{-6}$, and the CP-violating asymmetry $\mathcal{A}_{CP}(B^\mp \to \rho^\mp \pi^0) = 0.06 \pm 0.17(\text{stat})^{+0.04}_{-0.05}(\text{syst})$.

DOI: 10.1103/PhysRevLett.94.031801 PACS numbers: 13.25.Hw, 11.30.Er, 14.40.Nd

Recent precise measurements of $\sin 2\phi_1$ [1,2] confirm the prediction of the Kobayashi-Maskawa model [3] for CP violation. It is of great importance to test this theory further with complementary measurements, such as those of the other unitarity triangle angles ϕ_2 and ϕ_3 [4].

At the quark level, the decays $B \to \rho\pi$ occur via $b \to u$ tree diagrams and can be used to measure ϕ_2. However, because of the presence of $b \to d$ penguin (loop) diagrams, a model independent extraction of ϕ_2 from time-dependent CP-asymmetry measurements requires an isospin analysis of the decay rates of all the $\rho\pi$ decay modes [5]. The decay channels $B^+ \to \rho^0\pi^+$ [6] and $B^0 \to \rho^\pm\pi^\mp$ have already been measured [7]. Evidence for the $B^0 \to \rho^0\pi^0$ mode, which is expected to be small, has been reported by Belle [8] with a rate higher than an upper bound from *BABAR* [9]. The remaining decay mode, $B^+ \to \rho^+\pi^0$, has two neutral pions in the final state that make its measurement an experimental challenge. Recently, the *BABAR* group reported the observation of this mode [9].

In this Letter, we report measurements of the branching fraction and the CP-violating charge asymmetry for the $B^+ \to \rho^+\pi^0$ decay mode. The results are based on a 140 fb^{-1} data sample containing 152.0×10^6 B meson pairs collected with the Belle detector at the KEKB asymmetric-energy e^+e^- collider [10] operating at the $\Upsilon(4S)$ resonance ($\sqrt{s} = 10.58$ GeV).

The Belle detector is a large-solid-angle magnetic spectrometer that consists of a three-layer silicon vertex detector, a 50-layer central drift chamber (CDC), an array of aerogel threshold Čerenkov counters (ACC), a barrel-like arrangement of time-of-flight scintillation counters (TOF), and an electromagnetic calorimeter (ECL) comprising CsI(Tl) crystals located inside a superconducting solenoid coil that provides a 1.5 T magnetic field. An iron flux return located outside of the coil is instrumented to detect K_L mesons and to identify muons. The detector is described in detail elsewhere [11].

For charged pion and kaon identification, specific ionization measurements (dE/dx) from the CDC are combined with the responses of the ACC and TOF systems to form likelihoods L_π and L_K. We distinguish pions from kaons by applying selection requirements on the likelihood ratio, $L_\pi/(L_\pi + L_K)$. Similarly, electrons are identified by means of a likelihood based on ECL measurements, dE/dx information from the CDC, and the responses of the ACC.

The final state for the signal consists of a charged pion track and two $\pi^0 \to \gamma\gamma$ candidates. We select well-constrained charged tracks that are positively identified as pions and that are not consistent with the electron hypothesis. Candidate π^0 mesons are reconstructed from pairs of photons that have an invariant mass within $\pm 3\sigma$ of the nominal π^0 mass, where the photons are assumed to originate from the IP, and the π^0 resolution σ varies in the range 5.3–7.0 MeV depending on its momentum. The energy of each photon in the laboratory frame is required to be greater than 50 MeV for the ECL barrel region ($32° < \theta < 129°$) and 100 MeV for the ECL end cap regions ($17° < \theta < 32°$ or $129° < \theta < 150°$), where θ denotes the polar angle of the photon with respect to the beam line. The π^0 candidates are kinematically constrained to the nominal π^0 mass. In order to reduce the combinatorial background, we only accept π^0 candidates with momenta $p_{\pi^0} > 0.35$ GeV/c in the e^+e^- center-of-mass (c.m.) system. We select $\rho^+ \to \pi^+\pi^0$ decay candi-

dates with invariant masses in the range $0.62\ \mathrm{GeV}/c^2 < M(\pi^+\pi^0) < 0.92\ \mathrm{GeV}/c^2$.

$B^+ \to \rho^+\pi^0$ candidates are identified using the beam-constrained mass $M_{\mathrm{bc}} \equiv \sqrt{E_{\mathrm{beam}}^2 - p_B^2}$, and the energy difference $\Delta E \equiv E_B - E_{\mathrm{beam}}$, where E_{beam} is the c.m. system beam energy, and p_B and E_B are the c.m. system momentum and energy, respectively, of the B candidate. The ΔE distribution has a tail on the lower side caused by incomplete longitudinal containment of electromagnetic showers in the CsI crystals. We accept events in the region $M_{\mathrm{bc}} > 5.2\ \mathrm{GeV}/c^2$, $-0.4\ \mathrm{GeV} < \Delta E < 0.4\ \mathrm{GeV}$, and define signal regions in M_{bc} and ΔE as $5.27\ \mathrm{GeV}/c^2 < M_{\mathrm{bc}} < 5.29\ \mathrm{GeV}/c^2$ and $-0.20\ \mathrm{GeV} < \Delta E < 0.07\ \mathrm{GeV}$, respectively.

The continuum process $e^+e^- \to q\bar{q}$ ($q = u, d, s, c$) is the main source of background and must be strongly suppressed. We discriminate the signal from the background using event topology, which tends to be isotropic for $B\bar{B}$ events and jetlike for $q\bar{q}$ events. We use Monte Carlo (MC) simulated signal and continuum events to form a Fisher discriminant based on a set of modified Fox-Wolfram moments [12] that are verified to be uncorrelated with M_{bc}, ΔE, and variables considered later in the analysis. Another discriminating characteristic is θ_B, the c.m. system polar angle of the B flight direction. B mesons are produced with a $1 - \cos^2\theta_B$ distribution while continuum background events tend to be uniform in $\cos\theta_B$. Probability density functions (PDFs) derived from the Fisher discriminant and the $\cos\theta_B$ distributions are multiplied to form likelihood functions for signal ($\mathcal{L}_s$) and continuum ($\mathcal{L}_{q\bar{q}}$); these are combined into a likelihood ratio $\mathcal{R}_s = \mathcal{L}_s/(\mathcal{L}_s + \mathcal{L}_{q\bar{q}})$.

Additional discrimination is provided by the b-flavor tagging algorithm [13] developed for time-dependent analyses at Belle. We use the parameter r, which ranges from 0 to 1 and is a measure of the likelihood that the b flavor of the accompanying B meson is correctly assigned. Events with high values of r are well tagged and are less likely to originate from continuum production. We define a multidimensional likelihood ratio $\mathrm{MDLR} = \mathcal{L}_s^{\mathrm{MDLR}}/(\mathcal{L}_s^{\mathrm{MDLR}} + \mathcal{L}_{q\bar{q}}^{\mathrm{MDLR}})$, where $\mathcal{L}_s^{\mathrm{MDLR}}$ denotes the likelihood determined by the r-$\mathcal{R}_s$ two-dimensional distribution for signal and $\mathcal{L}_{q\bar{q}}^{\mathrm{MDLR}}$ is that for the continuum background. We make a requirement on the likelihood ratio $\mathrm{MDLR} > 0.9$ that maximizes the value of $S/\sqrt{S+B}$, where S is the number of signal events and B is the number of background events in the M_{bc} and the ΔE signal region. To determine S and B, we use a GEANT-based MC simulation [14]. The likelihood ratio requirement removes 99% of the continuum background while retaining 30% of the $B^+ \to \rho^+\pi^0$ signal.

Since $B^+ \to \rho^+\pi^0$ is a pseudoscalar $\to$ vector + pseudoscalar process, the ρ helicity angle θ_{hel}, defined as the angle between an axis antiparallel to the B flight direction and the π^+ flight direction in the ρ rest frame, has a $\cos^2\theta_{\mathrm{hel}}$ distribution. We require $|\cos\theta_{\mathrm{hel}}| > 0.3$ for further background suppression.

In the M_{bc}-ΔE signal region, about 8% of the events have multiple candidates. We choose the candidate that has the minimum sum of χ^2 for the mass constrained π^0 fits; in cases where candidates have the same χ^2, we select the candidate with the largest Fisher discriminant. The MC-determined efficiency with all selection criteria imposed is found to be 4.36%.

Backgrounds from B decays are investigated with MC simulation. For $b \to c$ decay processes, no signal-like peak is found in either the M_{bc} or the ΔE distribution. Among the much rarer charmless decays, the dominant backgrounds are from $B^0 \to \rho^+\rho^-$ decays with a missing low-momentum $\pi^\pm$, which populate the negative ΔE region, and $B^0 \to \pi^0\pi^0$ decays with an extra low-momentum $\pi^\pm$, which populate the positive ΔE region. Monte Carlo studies indicate that potential backgrounds from $B^+ \to a_1^+\pi^0$, $a_1^+ \to \rho^+\pi^0$ have ΔE and M_{bc} distributions similar to those for $B^0 \to \rho^+\rho^-$ decays and are accounted for by the latter component of the fit. In addition, the contamination from other possible rare B decays is taken into account in the systematic error.

We extract the $B^+ \to \rho^+\pi^0$ signal yield by applying an extended unbinned maximum-likelihood fit to the two-dimensional M_{bc}-ΔE distribution of the selected candidate events. The fit includes components for signal plus backgrounds from continuum events, $b \to c$ decays, $B^0 \to \rho^+\rho^-$, and $B^0 \to \pi^0\pi^0$. The PDFs for signal, $B^0 \to \rho^+\rho^-$ and $B^0 \to \pi^0\pi^0$, are modeled by smoothed two-dimensional histograms obtained from large MC samples. The signal PDF is adjusted to account for small differences observed between data and MC for high-statistics modes containing π^0's, i.e., $B^+ \to \overline{D}^0(K^+\pi^-\pi^0)\pi^+$ for M_{bc}, and $D^0 \to \pi^0\pi^0$ for ΔE, where we use π^0 mesons in similar momentum ranges to those from $B^+ \to \rho^+\pi^0$ decay. The continuum PDF is described by a product of a threshold (ARGUS) function [15] for M_{bc} and a first-order polynomial for ΔE, with shape parameters allowed to be free. Background from generic $b \to c$ decays is represented by an ARGUS function for M_{bc} and a third-order polynomial for ΔE with shape parameters determined from MC. In the fit, all normalizations are allowed to float, except for the $\pi^0\pi^0$ component, which is fixed at a MC-determined value based on recent Belle [12] and *BABAR* [16] measurements.

Figure 1 shows the final event sample and fit results. The six-parameter (four normalizations plus two shape parameters for continuum) fit gives a signal yield of 87.4 ± 14.9 events. The statistical significance of the signal, defined as $\sqrt{-2\ln(\mathcal{L}_0/\mathcal{L}_{\mathrm{max}})}$, where $\mathcal{L}_{\mathrm{max}}$ is the likelihood value at the best-fit signal yield and $\mathcal{L}_0$ is the value with the signal yield set to zero, is 8.1σ. The level of the $B^0 \to \rho^+\rho^-$ background determined from the fit is in good agreement with MC expectations based on a recent measurement of the branching fraction for this decay mode [17].

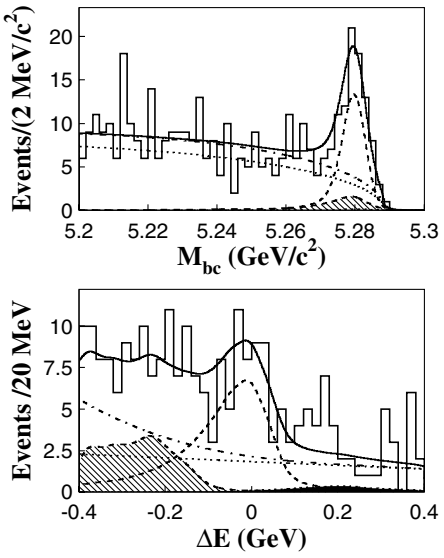

FIG. 1. The upper plot is the $M_{\rm bc}$ projection for events in the ΔE signal region $-0.20\ \text{GeV} < \Delta E < 0.07\ \text{GeV}$; the lower plot is the ΔE projection for events in the $M_{\rm bc}$ signal region $5.27\ \text{GeV}/c^2 < M_{\rm bc} < 5.29\ \text{GeV}/c^2$. The solid curve shows the results of the fit. The signal component is shown as a dashed line. The continuum background is shown as a dotted line. The sum of $b \to c$ and continuum components is shown as a dot-dashed line. The hatched (dark) histogram represents the $B^0 \to \rho^+\rho^-$ ($B^0 \to \pi^0\pi^0$) background.

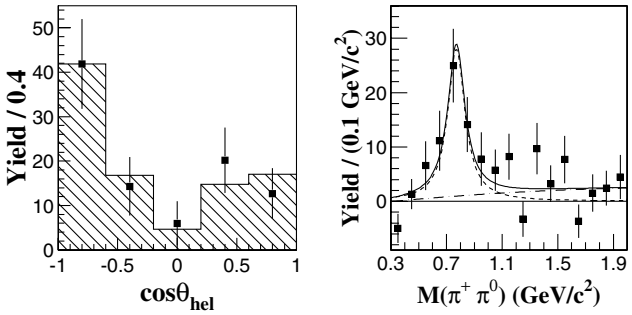

FIG. 2. The left plot is the $\cos\theta_{\rm hel}$ distribution for the ρ. Data points show the background-subtracted data; the hatched histogram shows the distribution for signal MC. The asymmetry in these distributions is due to the π^0 momentum requirement. The right plot is the $M(\pi^+\pi^0)$ distribution. Data points show the background-subtracted data, the dashed (dot-dashed) line is for the ρ signal (nonresonant) component of the fit, and the solid line is their sum.

To verify that the signal we observe is due to $B^+ \to \rho^+\pi^0$ decay, we examine the helicity and $M(\pi^+\pi^0)$ distributions. Figure 2 (left) shows the helicity angle distribution for signal yields determined from $M_{\rm bc}$-ΔE fits, which is consistent with that for signal MC events. The distribution for continuum is approximately flat.

Figure 2 (right) shows the signal yields extracted from $M_{\rm bc}$-ΔE fits applied to individual $M(\pi^+\pi^0)$ bins. A χ^2 fit to the background-subtracted $M(\pi^+\pi^0)$ distribution is performed with a ρ plus a nonresonant $\pi\pi$ component included. The ρ component is represented by a Breit-Wigner function with mass and width fixed at their known values [18]. The nonresonant $\pi\pi$ component is described by a second-order polynomial with shape parameters determined from $B^+ \to \pi^+\pi^0\pi^0$ MC events, where the final state particles are distributed uniformly over phase space. The fit gives the fraction of nonresonant decays in the $0.62\ \text{GeV}/c^2 < M(\pi^+\pi^0) < 0.92\ \text{GeV}/c^2$ ρ signal region as $(5.8 \pm 4.8)\%$. The nonresonant yield increased by 1σ is treated as a systematic uncertainty.

We consider systematic errors in the branching fraction of the decay $B^+ \to \rho^+\pi^0$ that are caused by uncertainties in the efficiencies of track finding, particle identification, π^0 reconstruction, continuum suppression, fitting, and a possible contribution from nonresonant decays. We assign a 1.2% error for the uncertainty in the tracking efficiency. This uncertainty is obtained from a study of partially reconstructed D^* decays. We also assign a 0.8% error for the particle identification efficiency that is based on a study of kinematically selected $D^{*+} \to D^0\pi^+$, $D^0 \to K^-\pi^+$ decays; an 8.0% systematic error for the uncertainty in the two-π^0 detection efficiency that is determined from data-MC comparisons of $\eta \to \pi^0\pi^0\pi^0$ with $\eta \to \pi^+\pi^-\pi^0$ and $\eta \to \gamma\gamma$; a 5.1% systematic error for continuum suppression that is estimated from a study of $B^+ \to \overline{D}{}^0\pi^+$, and $\overline{D}{}^0 \to K^+\pi^-\pi^0$ decays; a systematic error of $^{+4.3}_{-0.4}\%$ that is obtained from changes in signal yields that occur when each parameter of the fitting functions is varied by $\pm 1\sigma$; and a $^{+0}_{-10.5}\%$ systematic error to account for a possible contribution from nonresonant decays. Moreover, a 1% error due to backgrounds from charmless B decays other than $B \to \rho\rho$ and $B^0 \to \pi^0\pi^0$ is estimated by fitting the data with an additional component with the yield fixed at the MC-expected value. The change in the signal yield is taken as a systematic error to account for this contamination. We also include a 0.5% error for the uncertainty in the number of $B\bar{B}$ events in the data sample. The production rates of B^+B^- and $B^0\overline{B}{}^0$ pairs are assumed to be equal. We obtain the branching fraction

$$\mathcal{B}(B^+ \to \rho^+\pi^0) = (13.2 \pm 2.3(\text{stat})^{+1.4}_{-1.9}(\text{syst})) \times 10^{-6}.$$

Direct CP violation would be indicated by an asymmetry in the partial rates for $B^- \to \rho^-\pi^0$ and $B^+ \to \rho^+\pi^0$:

$$\mathcal{A}_{CP} \equiv \frac{\Gamma(B^- \to \rho^-\pi^0) - \Gamma(B^+ \to \rho^+\pi^0)}{\Gamma(B^- \to \rho^-\pi^0) + \Gamma(B^+ \to \rho^+\pi^0)}.$$

We perform a simultaneous fit to extract the charge asymmetry. The $B^\mp \to \rho^\mp\pi^0$ candidates are self-tagged, but this tagging is provided by a single low-momentum charged pion. About 9% of signal events are misreconstructed with the wrong charge using a pion from the other B. In the fit, we introduce asymmetry parameters for the

$B \to \rho\pi$ signal and also for the continuum and $b \to c$ backgrounds, and separate the wrong tagged fraction of the signal into an independent PDF, which is modeled by a smoothed two-dimensional histogram obtained from MC. Other PDFs are the same as used in the $M_{\rm bc}$-ΔE fit described earlier. In the fit all normalizations are allowed to float, except for the $\pi^0\pi^0$, and wrong tagged components, which are fixed at MC-determined values. The fit result is $A_{CP} = 0.06 \pm 0.17$.

The charge symmetry of the detector performance and reconstruction procedure is verified with a sample of $B^+ \to \overline{D}^0\pi^+$, $\overline{D}^0 \to K^+\pi^-\pi^0$ decays and their charge conjugates. We apply the same procedure that is used for $B^+ \to \rho^+\pi^0$ to select $B^+ \to \overline{D}^0\pi^+$ candidates and extract signal yields by fitting the ΔE distribution. We find 1478.8 ± 48.4 $B^- \to D^0\pi^-$ and 1584.8 ± 54.9 $B^+ \to \overline{D}^0\pi^+$ events, which corresponds to a direct CP-violating asymmetry of -0.03 ± 0.02. We assign 0.03 as the systematic error associated with detector and reconstruction effects. The systematic error due to the uncertainty in the wrong tagged fraction is found to be negligible. The systematic error associated with the fitting procedure is determined to be 0.01 by shifting each fitting function parameter by $\pm 1\sigma$ and taking the quadratic sum of the resulting changes in $\mathcal{A}_{CP}$. An error of $^{+0.00}_{-0.04}$ for nonresonant background is estimated by subtracting the nonresonant component, obtained from the fit to $M(\pi^-\pi^0)$ or $M(\pi^+\pi^0)$ and increased by $\pm 1\sigma$, from the B^- or B^+ signal yields. The change in $\mathcal{A}_{CP}$ is taken as the systematic error. A 0.01 systematic error due to the background from other rare B decays is assigned. The quadratic sum of these errors is taken as the total systematic error. We obtain a CP-violation charge asymmetry that is consistent with zero:

$$\mathcal{A}_{CP}(B^\mp \to \rho^\mp\pi^0) = 0.06 \pm 0.17(\text{stat})^{+0.04}_{-0.05}(\text{syst}).$$

In summary, we observe the decay $B^+ \to \rho^+\pi^0$ with a statistical significance of 8.1σ and measure its branching fraction. The results are consistent with those from the *BABAR* experiment [9]. This measurement provides one of the essential quantities to constrain ϕ_2 from an isospin analysis of $B \to \rho\pi$ decays. The measured charge asymmetry is consistent with zero.

We thank the KEKB group for the excellent operation of the accelerator, the KEK Cryogenics group for the efficient operation of the solenoid, and the KEK computer group and the NII for valuable computing and Super-SINET network support. We acknowledge support from MEXT and JSPS (Japan); ARC and DEST (Australia); NSFC (Contract No. 10175071, China); DST (India); the BK21 program of MOEHRD and the CHEP SRC program of KOSEF (Korea); KBN (Contract No. 2P03B 01324, Poland); MIST (Russia); MESS (Slovenia); NSC and MOE (Taiwan); and DOE (USA).

*On leave from Fermi National Accelerator Laboratory, Batavia, IL, 60510 USA

†On leave from Nova Gorica Polytechnic, Nova Gorica, Slovenia, 5000.

[1] Belle Collaboration, K. Abe *et al.*, Phys. Rev. Lett. **87**, 091802 (2001); Belle Collaboration, K. Abe *et al.*, Phys. Rev. D **66**, 071102 (2002).

[2] *BABAR* Collaboration, B. Aubert *et al.*, Phys. Rev. Lett. **87**, 091801 (2001); *BABAR* Collaboration, B. Aubert *et al.*, Phys. Rev. Lett. **89**, 201802 (2002).

[3] M. Kobayashi and T. Maskawa, Prog. Theor. Phys. **49**, 652 (1973).

[4] H. Quinn and A. I. Sanda, Eur. Phys. J. C **15**, 626 (2000).

[5] H. J. Lipkin, Y. Nir, H. R. Quinn, and A. E. Snyder, Phys. Rev. D **44**, 1454 (1991); A. E. Snyder, H. R. Quinn, Phys. Rev. D**48**, 2139 (1993).

[6] The inclusion of charge conjugate modes is implied unless stated otherwise.

[7] Belle Collaboration, A. Gordon *et al.*, Phys. Lett. B **542**, 183 (2002); *BABAR* Collaboration, B. Aubert *et al.*, Phys. Rev. Lett. **91**, 201802 (2003).

[8] Belle Collaboration, J. Dragic *et al.*, Phys. Rev. Lett. **93**, 131802 (2004).

[9] *BABAR* Collaboration, B. Aubert *et al.*, Phys. Rev. Lett. **93**, 051802 (2004).

[10] S. Kurokawa and E. Kikutani, Nucl. Instrum. Methods Phys. Res., Sect. A **499**, 1 (2003).

[11] Belle Collaboration, A. Abashian *et al.*, Nucl. Instrum. Methods Phys. Res., Sect. A **479**, 117 (2002).

[12] The Fox-Wolfram moments were introduced in G. C. Fox and S. Wolfram, Phys. Rev. Lett. **41**, 1581 (1978). The modified moments used in this Letter are described in Belle Collaboration, S. H. Lee *et al.*, Phys. Rev. Lett. **91**, 261801 (2003).

[13] H. Kakuno *et al.*, hep-ex/0403022.

[14] We assume a branching fraction of $\mathcal{B}(B^+ \to \rho^+\pi^0) = 10 \times 10^{-6}$ for this optimization.

[15] ARGUS Collaboration, H. Albrecht *et al.*, Phys. Lett. B **241**, 278 (1990).

[16] *BABAR* Collaboration, B. Aubert *et al.*, Phys. Rev. Lett. **91**, 241801 (2003).

[17] *BABAR* Collaboration, B. Aubert *et al.*, Phys. Rev. D **69**, 031102 (2004).

[18] K. Hagiwara *et al.*, Phys. Rev. D**66**, 010001 (2002); S. Eidelman *et al.*, Phys. Lett. B **592**, 1 (2004).